Journal of Biomechanics 83 (2019) 197–204

Contents lists available at ScienceDirect

Journal of Biomechanics

journal homepage: www.elsevier.com/locate/jbiomech
www.JBiomech.com

Muscle material properties in passive and active stroke-impaired muscle

Sabrina S.M. Lee [a,*], Kristen L. Jakubowski [a,b,d], Sam C. Spear [b], William Z. Rymer [b,c,d]

[a] Department of Physical Therapy and Human Movements Sciences, Northwestern University, Chicago, IL, USA
[b] Shirley Ryan AbilityLab, Chicago, IL, USA
[c] Department of Physiology, Northwestern University, Chicago, IL, USA
[d] Department of Biomedical Engineering, Northwestern University, Chicago, IL, USA

ARTICLE INFO

Article history:
Accepted 26 November 2018

Keywords:
Shear wave elastography
Muscle
Stroke
Stiffness
Ultrasound

ABSTRACT

Stroke survivors routinely experience long-term motor and sensory impairments. In parallel with neurological changes, material properties of muscles in the impaired limbs, such as muscle stiffness, may also change progressively. However, these stiffness measures are routinely derived from individual joint stiffness, representing whole muscle groups. Here, we use shear wave (SW) ultrasound elastography to measure SW velocity, as a surrogate measure of stiffness, to quantify material properties in individual muscles. Accordingly, the purpose of this study was to compare muscle material properties of the bicep brachii in stroke survivors and in age-matched control subjects by measuring SW velocity at rest and different voluntary activation levels. Our main findings show that at rest, the SW velocity was on average 41% greater in the paretic muscle compared the contralateral non-paretic muscle. The mean passive SW velocity across all subjects were 2.34 ± 0.41 m/s for the non-paretic side, 3.30 ± 1.20 m/s for the paretic side, and 2.24 ± 0.18 for controls. SW velocity was significantly different in muscles of the paretic and non-paretic side ($p < 0.001$), but not between muscles of the non-paretic and controls ($p = 0.47$). As voluntary activation increased, SW velocity increased non-linearly, with an average power fit of $r^2 = 0.83 \pm 0.09$ for the non-paretic side, $r^2 = 0.61 \pm 0.24$ for the paretic side, and $r^2 = 0.24 \pm 0.15$ for the healthy age-matched controls. In active muscle (10, 25, 50, 75, 100% maximum voluntary contraction), there was no significant difference in SW velocity between the non-paretic, paretic, and control muscles.

These findings suggest that stroke-impaired muscles have potentially altered muscle material properties, specifically stiffness, and that passive and active stiffness may contribute differently to total muscle stiffness.

1. Introduction

Changes in intrinsic muscle properties can occur in individuals who have had a stroke and often accompany long-term motor and sensory impairments. These changes include shortening of fascicles (Gao and Zhang, 2008), accumulation of connective tissue (Lieber and Ward, 2013), and increased passive joint and muscle stiffness (Gao and Zhang, 2008; Katz and Rymer, 1989; Lee et al., 2015). In addition to decreased muscle mass, the force-length and force-velocity relationships may be altered such that force generation is impaired. Muscle material properties also play a role in force generation; however, little is known about the material properties of stroke-impaired muscle.

Quantifying muscle material properties, such as stiffness and elastic modulus, is challenging. There has been much work on quantifying total joint stiffness (Chardon et al., 2010; de Vlugt et al., 2010; Roy et al., 2011; Sinkjær and Magnussen, 1994), but these measurements encompass many elements including the joint capsule, surrounding ligaments, and all muscles crossing the joint. Furthermore, stiffness is routinely estimated indirectly by joint torque measurements (Gao and Zhang, 2008), kinematic protocols (Lamontagne et al., 2000), calculating limb dynamics (Sinkjær and Magnussen, 1994), or measuring force generation during tendon indentation (Chardon et al., 2010). Other stiffness measures of spastic muscle include intraoperative measurements of sarcomere and fascicle forces (Lieber et al., 2003). While these various measurements are invaluable in determining the stiffness at the fiber or fascicle level, they do not provide information at the whole muscle level and are also highly invasive.

Shear wave (SW) ultrasound elastography is an alternative method for quantifying material properties and most recently

* Corresponding author at: Department of Physical Therapy and Human Movement Sciences, Chicago, IL 60611, USA.
E-mail address: s-lee@northwestern.edu (S.S.M. Lee).

https://doi.org/10.1016/j.jbiomech.2018.11.043
0021-9290/

has been successfully applied to a variety of muscles in both healthy young adults (Bouillard et al., 2012; Lapole et al., 2015; Nordez and Hug, 2010; Sasaki et al., 2014; Yoshitake et al., 2014), and in clinical populations such as stroke and cerebral palsy (Lee et al., 2015, 2016). Supersonic shear imaging (SSI) uses acoustic radiation forces to induce shear waves within soft tissue and SW propagation is tracked using ultra-fast ultrasonic imaging (Bercoff et al., 2004). SW velocity is related to the elastic modulus of the tissue such that SWs will travel faster in a stiffer material (Brandenburg et al., 2014). In healthy young adults, it has been shown that SW velocity is dependent on activation level in various muscles such as the gastrocnemius (Chernak et al., 2013), bicep brachii (Bouillard et al., 2012; Lapole et al., 2015; Nordez and Hug, 2010; Sasaki et al., 2014; Yoshitake et al., 2014), and tibialis anterior (Sasaki et al., 2014). In previous work, we have shown that SW velocity of passive paretic bicep brachii is greater compared to non-paretic muscle in stroke survivors with hemiparesis (Lee et al., 2015). However, little is known about the effect, if any, stroke has on the SW velocity in muscle under active conditions. Thus, the aim of this study was to use SW ultrasound elastography to determine if there are differences in SW velocity in passive and in active paretic and non-paretic muscle of individuals who have had a hemispheric stroke, and to compare these measurements with muscles of healthy age-matched individuals.

2. Methods

2.1. Subjects

Fourteen individuals with chronic stroke-induced hemiparesis participated in this study (nine females and five males, mean (SD) age: 58.9 (7.4) years; height: 1.68 (0.10) m; body mass: 85.5 (18.2) kg; time post stroke: range: 2.1–27.3, mean (SD): 10.2 (8.4) years; Fugl-Meyer: range: 4–48, mean (SD): 19.6 (15.0); modified Ashworth: range 0–3; modified Tardieu: 1–3 muscle quality, 62°-145° catch angle for three speeds). Eight age- and sex-matched control individuals with no history of neurological or muscular disorders participated in this study (four females and four males, mean (SD) age: 57.4 (7.4) years; height: 1.68 (0.11) m; body mass: 75.0 (12.0) kg). All subjects gave informed consent prior to testing and Northwestern University's Institutional Review Board approved all procedures.

2.2. General set up

Participants were seated upright in a Biodex chair (Biodex Medical System, Inc. Shirley, NY) with their upper arm resting on a plastic support. To standardize hand position and to minimize activity of unrecorded muscles, the forearm was secured in a fiberglass cast with the wrist and forearm held in a neutral position (flexion-extension and supination-pronation) and placed in a ring-mount interface that was mounted on the table. The shoulder was positioned such that the humerus was abducted 45° and the elbow positioned at 90°. Torque and force at the wrist were also measured using a six degrees-of-freedom load cell (ATI, Apex, NC). Surface electromyogram data were collected from the long and short heads of the bicep brachii and triceps brachii using bipolar electrodes with the signal amplified by a gain of 1000 (Bagnoli Delsys, Inc,. Boston, MA).

2.3. Ultrasound

Ultrasound images were captured using a SW ultrasound elastography system (Aixplorer SuperSonic Imagine, Aix en Provence, France) (Bercoff et al., 2004). We collected images of the biceps brachii of the paretic and non-paretic side, and the dominant arm in control subjects (three images per % maximum voluntary contraction (MVC)). Technical details of this ultrasound technology have been described previously (Bercoff et al., 2004). The transducer was positioned at the mid-belly region of the long head of the bicep brachii and aligned with the fascicles as viewed from the B-mode image. A customized neoprene sleeve held the transducer in place to minimize undesired probe motion. The SW velocity map region of interest (ROI) (12 mm by 12 mm, Fig. 1) was manually placed in between the superficial and deep aponeuroses.

2.4. Procedure

Once secured in the set-up, subjects were given five minutes to practice contracting their biceps, by performing isometric elbow flexion tasks. Three MVC trials of three seconds were performed to obtain the maximum EMG and torque. Subjects performed isometric elbow flexion contractions at different activation levels (0, 10, 25, 50, 75, 100% of torque MVC), while ultrasound images of the bicep brachii were captured. The order of MVC trials and paretic/non-paretic sides were randomized. Subjects were given real-time visual feedback of their %MVC torque to match with desired %MVC torque target set by the experimenter. When the subject achieved the desired level of torque, an ultrasound image was captured. To prevent fatigue, each trial lasted no longer than eight seconds and subjects were given rest as needed. Three trials of each activation level were conducted with one image captured per trial. An external trigger was used to record when the ultrasound image was captured, allowing the torque and EMG data to be synced with the SW data.

2.5. Data analysis – Ultrasound

Custom-written software in MATLAB (Mathworks, Natick, USA) adapted from the propriety company software was used in this study. In the company software, mean SW velocity is calculated from a circular region with varying diameters selected by the experimenter from the 12 mm by 12 mm ROI (Fig. 1). In our analysis, all the values from the ROI were used except for areas outside of the muscle belly, which were manually cropped. This way, the maximal area for including SW velocity values was achieved. The spatial average of SW velocity was then calculated across the cropped ROI for each trial. Further details of this analysis are described elsewhere (Lee et al., 2015). Thus, we had one SW velocity value per trial. The maximum SW velocity the system is capable of measuring was 16 m/s; thus, if any value within the ROI exceeded 16 m/s, the trial was discarded. A total of 29 trials were discarded.

We have previously tested the repeatability and reliability of the SW velocity measurements. In these analyses, three unimpaired subjects and three stroke survivors were tested twice on separate days. SW velocity was reliable and repeatable (unimpaired: ICC = 0.932, CV = 4.5%; non-paretic side: ICC = 0.821 m, CV = 6.5%; paretic side: ICC = 0.715, CV = 9.2%). Inter-day reliability of the SSI technique in unimpaired muscle has also been previously reported (Lacourpaille et al., 2012; Yoshitake et al., 2014). Previous work has reported inter-day reliability in the medial gastrocnemius muscle of the non-paretic side, but found that measures had low reliability in muscle of the paretic side (Mathevon et al., 2018).

2.6. Data analysis – EMG/Torque

Torque data were processed with a 20 Hz low-pass filter. EMG data from the biceps brachii were bandpass filtered (20–450 Hz) and the rectified EMG signal was smoothed using a moving average

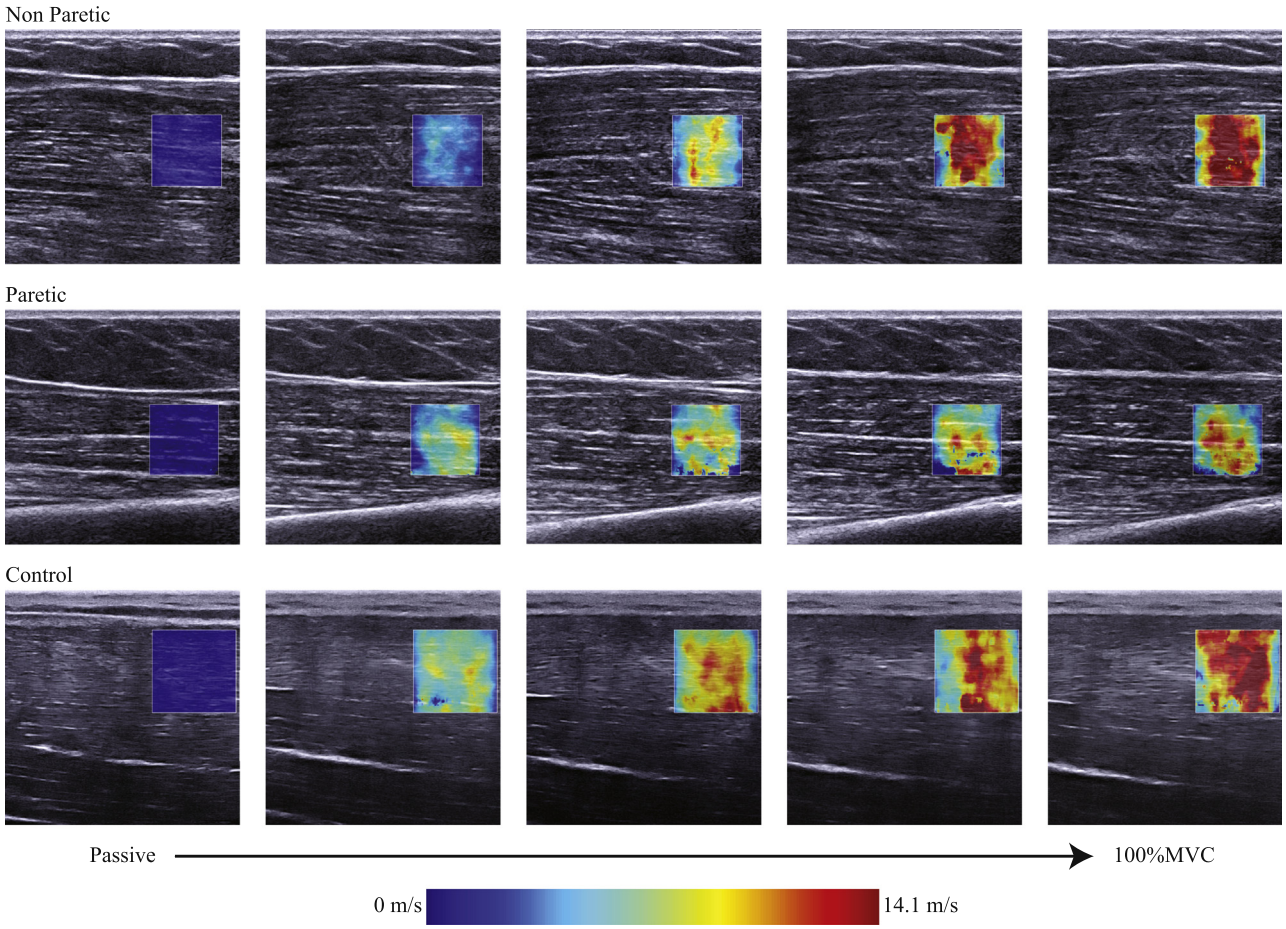

Fig. 1. Shear wave velocity maps superimposed on B-mode ultrasound images of biceps brachii of the non-paretic (top) and paretic (middle) side of a representative stroke subject and of an age-matched control subject from rest to maximum voluntary contraction.

filter (500 ms). To obtain the average torque and EMG for each trial, the filtered signals were averaged over a 500 ms window around the time of image capture. Each signal was normalized by MVC, calculated as the mean of the three highest intensity trials. Taking into account the inherent noise of EMG collection, a threshold noise value of 3 μV RMS EMG which is within a single standard deviation of 2.5 μV RMS, the noise level of the electrode (Merletti and Parker, 2004). Any trial where the EMG signal was one standard deviation greater than the threshold value was excluded from the analysis for the passive condition. Specifically, for two stroke subjects (paretic side) and one control subject, the EMG signal for all the passive trials was higher than the noise threshold; thus, those trials were not included in the analysis to determine the passive SW velocity. Those trials were included in the analysis for the active conditions. As EMG data from both heads of the biceps brachii were similar, results presented here are from the long head of the biceps brachii.

To compare the SW velocity at different levels of activation between sides and the control subjects, the SW velocity - %MVC EMG and torque data were first fit to linear, quadratic, and first order power equations for each subject (Fig. 3). The coefficient of determination (R^2) was calculated to assess the goodness of fit. There was no significant difference in R^2 values between quadratic and power equations; however, both had higher R^2 values compared to linear fits. While the quadratic fit had the highest R^2 values, in some subjects, the SW velocity peaked prior to maximal activation, and would subsequently decrease with increased activation. Not only was this relationship not observed experimentally, but it is also not physiologically congruent with cross-bridge dynamics. Therefore, using the power equations for each subject (Tables 1 and 2), SW velocity values were extrapolated at different levels of activation (10, 25, 50, 75, and 100 %MVC) for each subject.

2.7. Clinical tests

Clinical tests and physical measurements were conducted by a licensed physical therapist. The modified Ashworth (Pandyan et al., 1999) and the modified Tardieu (Singh et al., 2011) were used for evaluating spasticity. Fugl-Meyer assessment of motor recovery after a stroke was used to test motor impairment (Gladstone et al., 2002). Physical examination measurements included passive and active elbow range of motion. Passive range of motion measurements involved the physical therapist moving the limb from maximum flexion to extension while the muscles were at rest. Joint angles were measured using a manual goniometer. For active range of motion measurements, the subject was instructed to actively move the limb to maximum flexion and extension. Elbow angles were defined as the angle between the humerus and the ulna (flexion 0° to extension 180°).

2.8. Statistical analysis

We used a linear mixed effects model to compare passive SW velocity between the non-paretic, paretic, and healthy age matched controls. SW velocity was treated as the response variables, side (NP, P, and controls) was nominal and nested with sub-

Table 1
Power fit equations for shear wave velocity and percent maximum voluntary contraction using electromyography for individuals with stroke (paretic and non-paretic side) and age-matched controls. $y = a * x^b$.

Subject	Stroke Subjects					
	Non-paretic			Paretic		
	a	b	R^2	a	b	R^2
1	6.31	0.13	0.71	5.08	0.20	0.48
2	3.55	0.28	0.92	4.50	0.19	0.64
3	3.09	0.32	0.90	2.14	0.31	0.82
4	2.63	0.31	0.88	3.43	0.27	0.77
5	1.95	0.30	0.83	3.94	0.15	0.76
6	2.83	0.33	0.83	5.12	0.15	0.68
7	2.87	0.30	0.85	2.55	0.32	0.78
8	2.08	0.34	0.90	6.29	0.05	0.08
9	0.36	0.71	0.89	1.73	0.44	0.93
10	0.92	0.44	0.62	3.77	0.18	0.26
11	3.15	0.34	0.81	3.25	0.24	0.64
12	2.54	0.24	0.71	2.29	0.20	0.68
13	2.21	0.41	0.88	3.60	0.22	0.36
14	2.28	0.34	0.89	4.08	0.19	0.74
Control subjects						
Subject		a		b		R^2
1		1.96		0.28		0.49
2		4.13		0.27		0.91
3		2.15		0.31		0.87
4		3.94		0.26		0.96
5		6.14		0.17		0.84
6		3.25		0.25		0.90
7		1.77		0.46		0.75
8		3.37		0.29		0.87

Table 2
Power fit equations for shear wave velocity and torque for individuals with stroke (paretic and non-paretic side) and age-matched controls. $y = a * x^b$.

Subject	Stroke Subjects					
	Non-paretic			Paretic		
	a	b	R^2	a	b	R^2
1	5.68	0.15	0.46	2.56	0.34	0.89
2	2.46	0.35	0.90	4.49	0.19	0.60
3	0.94	0.58	0.94	1.96	0.33	0.82
4	3.50	0.23	0.71	4.97	0.18	0.66
5	1.52	0.35	0.77	2.99	0.20	0.79
6	3.75	0.27	0.68	6.43	0.11	0.53
7	7.26	0.06	0.09	5.08	0.15	0.51
8	2.94	0.27	0.75	2.78	0.25	0.44
9	0.62	0.59	0.90	2.90	0.33	0.95
10	0.20	0.76	0.57	5.22	0.11	0.39
11	2.99	0.34	0.93	3.44	0.23	0.64
12	2.75	0.22	0.78	2.48	0.17	0.48
13	2.98	0.32	0.94	6.30	0.11	0.72
14	2.65	0.31	0.86	4.51	0.17	0.77
Control subjects						
Subject		a		b		R^2
1		2.76		0.20		0.32
2		2.44		0.35		0.88
3		0.99		0.46		0.78
4		5.03		0.16		0.19
5		5.34		0.19		0.76
6		1.91		0.36		0.87
7		4.59		0.22		0.29
8		2.39		0.35		0.37

ject (random effect). A linear mixed effects model was also used to examine the effect of activation on SW velocity. Again, SW velocity was the response variable, activation level was considered a continuous variable, and side (NP, P, and control) was nominal and nested with subject (random effect). To then compare if SW velocity was significantly different between side at different levels of activation, the fitted SW velocity values were treated as the response variables, activation level was nominal, and side (NP, P, and control) was nominal and nested with subject (random effect). Lastly, a linear mixed effects model was used to examine the effect of torque on SW velocity. SW velocity was the response variable, torque, as a function of its maximum, was considered a continuous variable, and side (NP, P, and control) was nominal and nested with subject (random effect). Bonferroni corrections were used on all models with multiple comparisons. Linear regression analysis was conducted to evaluate correlations between SW velocity of both passive and active muscle, and clinical tests. Significance was set at $p \leq 0.05$. All statistics where performed either in MATLAB or Minitab 17 (State College, PA).

3. Results

3.1. Shear wave velocity – passive muscle

There were significant differences in the passive SW velocity between the paretic, non-paretic, and controls ($p < 0.001$). The mean passive SW velocity across all subjects were 2.34 ± 0.41 m/s for the non-paretic side, 3.30 ± 1.20 m/s for the paretic side, and 2.24 ± 0.18 for controls, with the paretic being 41.1% greater than the non-paretic (Fig. 2). A post hoc analysis indicated that while there was no significant difference between the passive SW velocity in muscles of non-paretic and controls ($p = 0.47$), the paretic side had significantly higher passive SW velocity than either of the other groups ($p < 0.001$).

3.2. Shear wave velocity – active muscle

When investigating the overall effect of activation on SW velocity, we found that activation level, as well as the interaction between activation level and side were significant ($p < 0.01$). A post hoc analysis revealed that the slope of the SW velocity versus activation level relationship was significantly different between sides, where the paretic side was significantly lower than both the non-paretic side ($p = 0.008$), and healthy controls ($p = 0.01$). Since, this relationship was found to be significant, further investigation into whether SW velocity was significant at different levels of activation was performed. As activation level increased, measured by %MVC EMG, SW velocity increased non-linearly with an average power fit across all subjects of $r^2 = 0.83 \pm 0.09$ for the non-paretic side, $r^2 = 0.61 \pm 0.24$ for the paretic side, and $r^2 = 0.24 \pm 0.15$ for

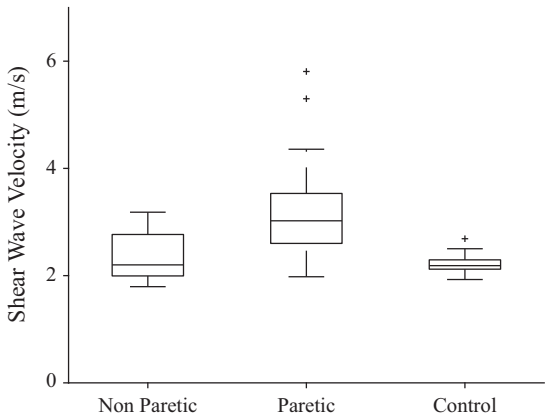

Fig. 2. Boxplot of shear wave velocity in biceps brachii muscles under passive conditions of the non-paretic and paretic sides of individuals post-stroke and age-matched controls. Box represents the middle 50% of the data with the center lines representing the median. Upper and lower whiskers represent the lower 25% and upper 25% of the distribution, respectively.

the healthy age-matched controls (Fig. 4). Using the power fit equations (Table 1), the SW velocity was calculated at 10, 25, 50, 75 and 100% MVC EMG. Both activation level and the interaction between activation level and arm (non-paretic, paretic, and healthy control, had significant influence over SW velocity ($p < 0.001$). However, the post hoc analysis revealed that when investigating specific interactions, none were significant ($p > 0.003$, corrected alpha value).

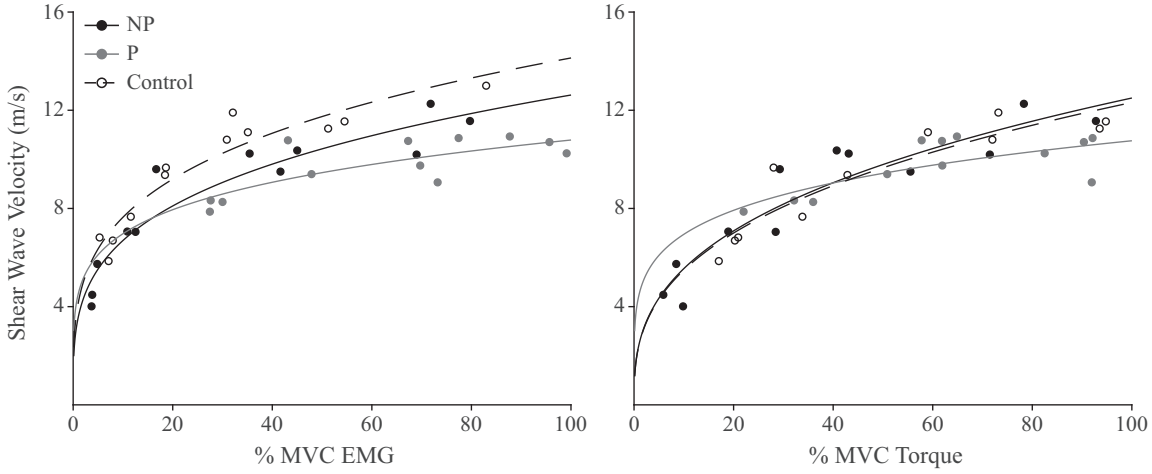

Fig. 3. From a representative subject, the relationship between shear wave velocity and % MVC from EMG for the non-paretic side (NP, solid black line, black dots) the paretic side (P, solid grey line, grey dots), and healthy age-matched control (dashed line, white dots) (left). From a representative subject, the relationship between shear wave velocity and torque for the non-paretic side (NP, solid black line, black dots) the paretic side (P, solid grey line, grey dots), and healthy age-matched control (dashed line, white dots) (right).

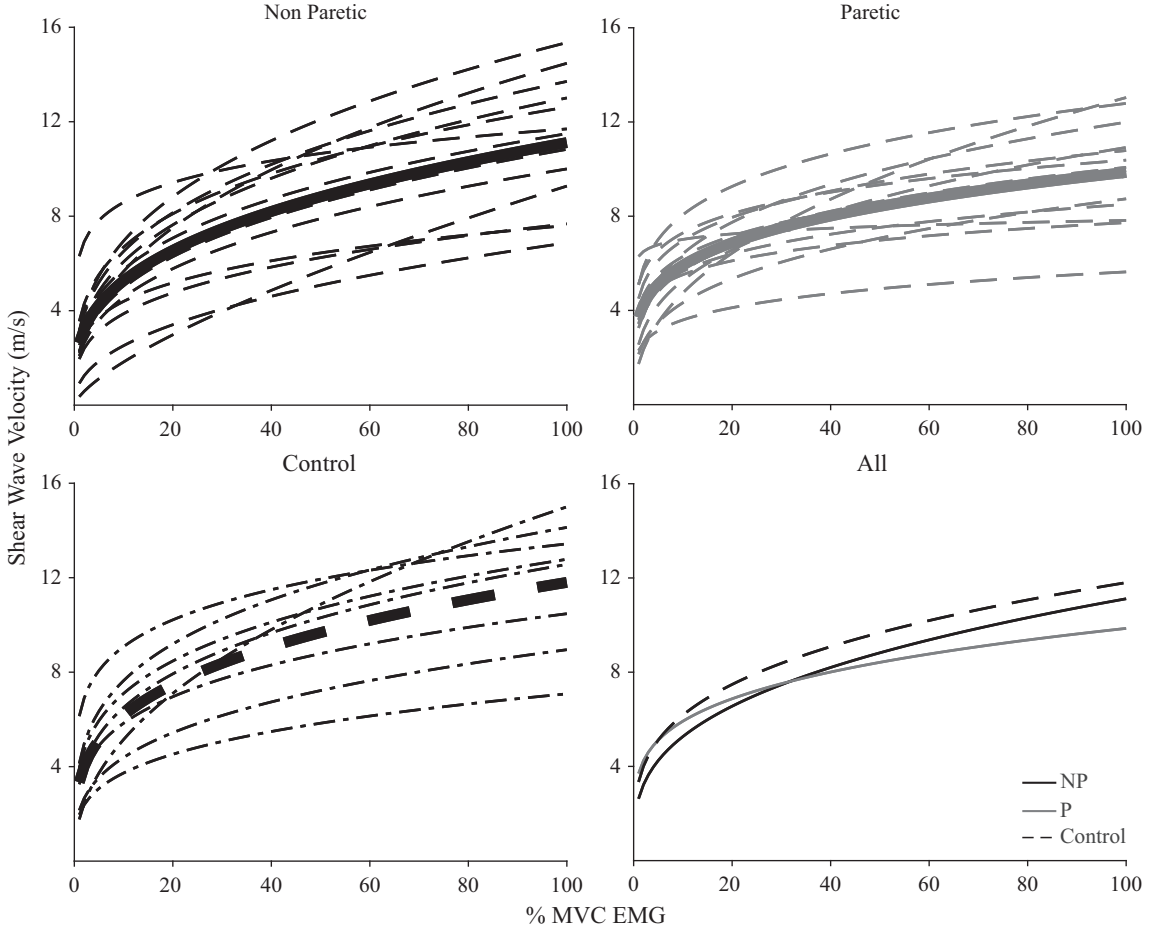

Fig. 4. Individual (dotted lines) and mean (solid lines) of the extrapolated fits (1–100%) for shear wave velocity and % maximum voluntary contraction (MVC) as expressed calculated from electromyography (EMG) of the non-paretic side (NP, solid black line) the paretic side (P, solid grey line), and healthy age-matched controls (dashed line) biceps brachii under active conditions. Each line represents one subject, except for 'All' (bottom right) which is an average across all subjects. Power functions of individual subjects are shown in Tables 1 and 2.

There was a significant difference in the SW velocity at low levels of activation between non-paretic, paretic, and controls; however, once activation level increased to 75%, there was no significant difference (10%-25%MVC $p = 0.010$, 75–100%MVC $p = 0.409$, Fig. 4). Similar to the SW velocity - EMG relationship, the SW velocity increased non-linearly as torque increased with an average power fit across all subjects of $r^2 = 0.73 \pm 0.23$ for non-paretic, $r^2 = 0.66 \pm 0.17$ for paretic, and $r^2 = 0.56 \pm 0.29$ for controls (Fig. 5).

3.3. Clinical assessments

We found that the non-paretic arm had significantly greater passive and active elbow range of motion than the paretic arm (mean (SD), non-paretic: active: 180 (5)° to 44 (11)°; passive: 182 (4)° to 37 (6); paretic: active: 145 (27)° to 59 (10)°; passive 175 (8)° to 45 (7)°; active: $p = 0.006$, passive $p = 0.001$). Passive SW velocity on the paretic side was correlated with the modified Ashworth (elbow extensors) ($p = 0.044$). No significant correlations were found between any of the clinical tests and active SW velocity.

4. Discussion

Using SW ultrasound elastography, we investigated changes in muscle material properties that may develop after a hemispheric stroke in passive and active muscle. We found that there was a significant difference between the mean SW velocity of passive stroke-impaired muscle and non-impaired muscle, measured from either the contralateral side or from age-matched controls. In contrast, there were no differences in the SW velocity at different voluntary activation levels.

Interpreting SW velocity values in muscle with regards to material properties is not straightforward. Firstly, assumptions for relating SW velocity to the elastic modulus include (a) isotropy, (b) homogeneity, and (c) negligible viscosity. Muscle is neither isotropic or homogenous and has known viscous properties. In addition, relating SW velocity to elastic modulus and stiffness is difficult as tension influences SW velocity (Koo and Hug, 2015). This latter consideration is important especially since both muscle stiffness and tension increase with increased muscle length and activation. Thus, the exact relationships between SW velocity, elastic modulus, tension, and stiffness in muscle are not well characterized, and caution is advised when interpreting SW velocity. Here, we simply state that increased SW velocity suggests changes in material properties that are likely related to changes in muscle stiffness.

Our finding of increased SW velocity in passive stroke-impaired biceps brachii muscle indicates that changes may occur within muscle following a stroke that contribute to changes in material properties. We build upon previous work where we observed increased passive SW velocity in paretic muscle compared to muscle of age-matched controls (Lee et al., 2015). This increase was also strongly correlated with increased echogenicity, a measure

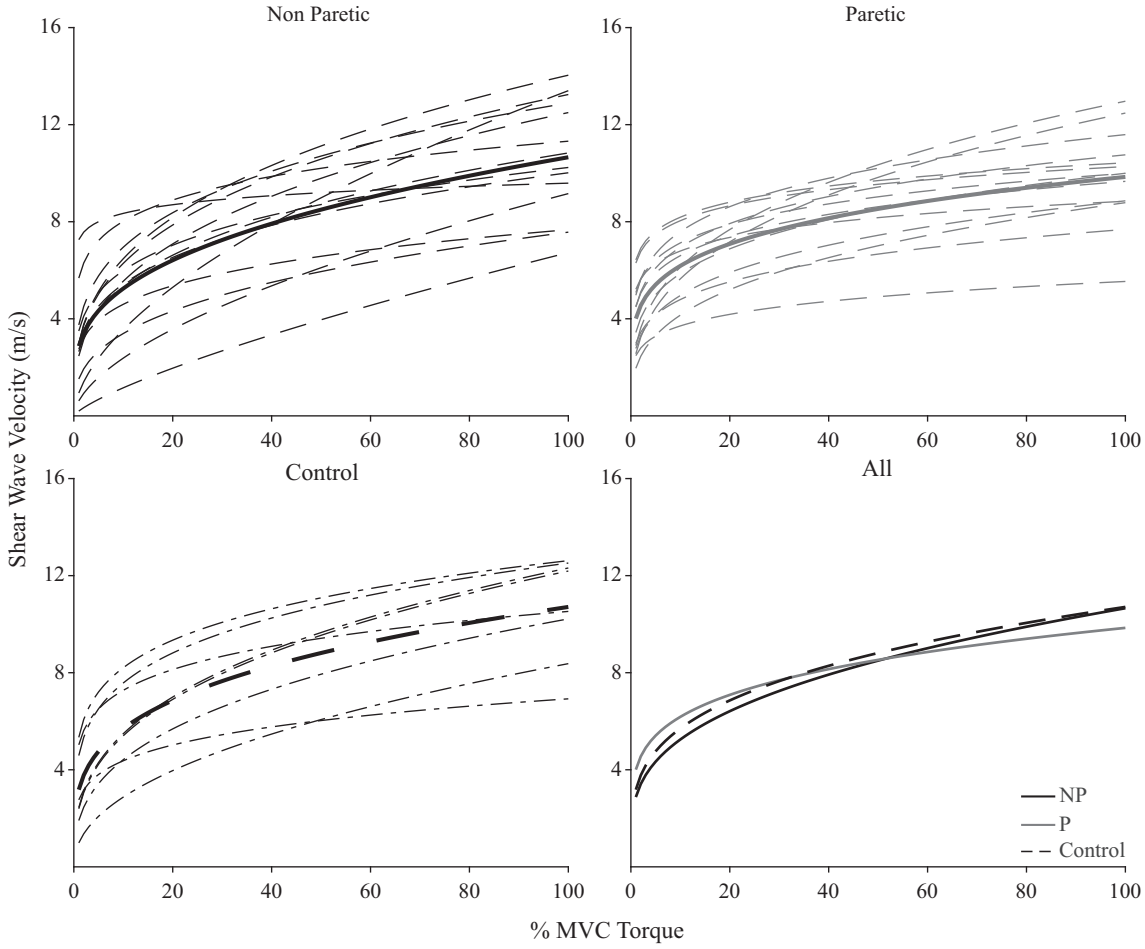

Fig. 5. Individual (dotted lines) and mean (solid lines) of the extrapolated fits for shear wave velocity and % maximum voluntary contraction (MVC) as expressed calculated from torque of the non-paretic side (NP, solid black line) the paretic side (P, solid grey line), and healthy age-matched controls (dashed line) biceps brachii under active conditions. Each line represents one subject, except for 'All' (bottom right) which is an average across all subjects. Power functions of individual subjects are shown in Tables 1 and 2.

to detect changes in muscle composition such as connective tissue and fatty infiltration (Lee et al., 2015). Sources of increased passive stiffness include structures containing collagen such as the extracellular matrix (ECM) (Lieber and Ward, 2013) comprised of the epimysium and perimysium (Magid and Law, 1985), and intracellular proteins such as titin (Fortuna et al., 2011; Herzog et al., 2015; Lieber and Ward, 2013).

While SW velocity was dependent on activation level, there were no differences in SW velocity at matched levels of activation between muscles of paretic and non-paretic sides, and controls. The SW velocity measured here reflects the material properties comprised of both active and passive components. If we assume that SW velocity reflects stiffness measured in the muscle, and tension contributes minimally, by taking measurements of the muscle at rest, we assume that only the passive component is contributing to the total stiffness. While it is believed that active stiffness is primarily due to actin-myosin cross-bridge attachment (Ford et al., 1981), the effect of the motor recruitment strategy, fiber type, or material properties has on active stiffness is unknown. There is evidence that following movement, the number of cross-bridges is temporarily decreased resulting in thixotropy (Altman et al., 2015; Herzog et al., 2015; Lakie et al., 1984). Thixotropy in muscle occurs when stiffness, from the fiber level to whole muscle level decreases after a stretch, but returns to initial value after a resting period (Buchthal, 1951). This history-dependent stiffness has been suggested to assist the role of muscle to resist externally applied forces (Lakie et al., 1984) such that muscle stiffness is increased under passive conditions to resist unexpected externally applied forces, but when active, the stiffness is reduced as this stability is not needed. Titin filaments have also been suggested to contribute to thixotropy (Minajeva et al., 2001). The contribution of titin to muscle stiffness increases dramatically under active conditions by changing its material properties and changing its free spring length (Herzog et al., 2015). However, little is known about the effects of stroke on myosin-actin interactions, as well as titan.

As we cannot accurately determine contribution of active stiffness to total stiffness with SW velocity, we can only speculate on our observations of different SW velocity under passive conditions between muscles of paretic and non-paretic sides, and controls, but no difference under matched levels of activation. Two possible explanations for our findings include: (1) the contribution of active components to total stiffness is much greater than the contribution from passive components, especially at higher levels of activation, and/or (2) stroke survivors have decreased active stiffness. In the first scenario, any contribution of passive stiffness to total stiffness is negligible once the muscle is activated, and as such, the increase in passive stiffness of stroke-impaired muscle is inconsequential when measured in an active muscle. This may simply be an expression of the relative mass of contractile versus non-contractile tissue in a large muscle, such as the biceps brachii.

There is published evidence of a leftward shift of the force-length curve of stroke-impaired muscle (Gao and Zhang, 2008). All of these changes could reduce the number of available attached cross-bridges resulting in decreased active stiffness. With the reduction in active stiffness of stroke-impaired muscle, the total stiffness would then be similar to non-impaired muscle. Further work is needed to investigate active stiffness at similar muscle lengths instead of at similar angles, ensuring that comparisons are being made at similar locations along the force-length curve. As mentioned previously, tension can influence SW velocity. Thus, changes in muscle properties such as the ECM, contractile tissue, or intracellular proteins that also affect force generation could contribute the differences in SW propagation in impaired muscle.

Another possibility explaining decreased active stiffness is that the intrinsic properties of the actin and myosin filaments are altered. There is evidence that the thick and thin filaments contribute to stiffness such that 49% of sarcomere compliance of active muscle is due to thin filaments (Kojima et al., 1994), while the remainder is due to the cross-bridges and thick filaments. There is some evidence demonstrating that filament stiffness may be substantially greater than that of cross-bridges as the stiffness of tetanized, single, intact muscle fibers is correlated with filament overlap (Ford et al., 1981; Huxley and Simmons, 1971). Thin filaments may have a more active role in contraction than as rigid force transmitters, as demonstrated by the bending motions of actin (Takebayashi et al., 1977). However, little is known about the intrinsic properties of the thick and thin filaments in stroke-impaired muscle. As mentioned above, titin contributes to muscle stiffness under activation; the passive force of titin effects the force-length curve such that there is an increase in stiffness at a given sarcomere length (Herzog et al., 2015) Thus, any changes in the properties of titin and its interaction with actin and myosin due to stroke may affect the material properties of the muscle.

For comparison with previous studies of shear modulus and muscle activation, we converted our SW velocity values to shear modulus (SW velocity^2 * density, where density for muscle is 1000 kg m^{-3}, (Bercoff et al., 2004; Brandenburg et al., 2014; Muthupillai et al., 1995). Our results of non-impaired muscle are similar to those reported for submaximal <10% MVC, <30%MVC (Nordez and Hug, 2010), <60% MVC (Yoshitake et al., 2014), and during maximum contractions (Lapole et al., 2015).

Limitations of this work include that the maximum SW velocity measured by the ultrasound system is 16 m/s; thus, for a limited number of subjects, we were only able to collect data during contractions up to 70% as some SW velocity values within the ROI would exceed 16 m/s. Additionally, measurements were only obtained at 90° elbow flexion for all subjects where resting slack length and fascicle length could differ between non-paretic, paretic, and controls. To be conservative that there was no muscle activity under passive conditions, we used the noise threshold of our EMG system as a criterion; however, it is possible that there were low levels of activation below the threshold. Also, only the biceps brachii of the dominant limb of the control subjects was tested; however, in a small subset of non-impaired individuals (n = 3), the difference in SW velocity between the dominant and non-dominant hand was similar to the standard deviation between trials of the same muscle.

5. Conclusion

These results demonstrate that although SW velocity is increased in stroke-impaired biceps brachii muscle under passive conditions, indicating changes in material properties, this difference between muscle of the paretic and non-paretic sides, and age-matched controls is not present in active muscle. This suggests that sources of passive and active components related to stiffness may be altered differently post-stroke. Providing clinicians with patient specific information on the material properties of muscle will allow clinicians to create patient specific interventions. For example, patients who presents with large increases in passive stiffness, but not active stiffness may not be ideal candidates for neurotoxic treatment.

Conflict of interest statement

The authors have no conflicts of interest to declare.

Acknowledgements

This work was funded by NIDDR H133P110013 and the Falk Medical Research Trust.

References

Altman, D., Minozzo, F.C., Rassier, D.E., 2015. Thixotropy and rheopexy of muscle fibers probed using sinusoidal oscillations. PLoS ONE 10, e0121726.

Bercoff, J., Tanter, M., Fink, M., 2004. Supersonic shear imaging: a new technique for soft tissue elasticity mapping. IEEE Trans Ultrason Ferroelectr Freq Contr 51, 396–409.

Bouillard, K., Nordez, A., Hodges, P.W., Cornu, C., Hug, F., 2012. Evidence of changes in load sharing during isometric elbow flexion with ramped torque. J. Biomech. 45, 1424–1429.

Brandenburg, J.E., Eby, S.F., Song, P., Zhao, H., Brault, J.S., Chen, S., An, K.N., 2014. Ultrasound elastography: the new frontier in direct measurement of muscle stiffness. Arch. Phys. Med. Rehabil. 95 (11), 2207–2219

Buchthal, F., 1951. The Rheology of the Cross Striated Muscle Fibre: With Particular Reference to Isotonic Conditions. I kommission hos Munksgaard.

Chardon, M.K., Suresh, N.L., Rymer, W.Z., 2010. Year An evaluation of passive properties of spastic muscles in hemiparetic stroke survivors. Annual International Conference of the Engineering in Medicine and Biology Society (EMBC). IEEE.

Chernak, L.A., DeWall, R.J., Lee, K.S., Thelen, D.G., 2013. Length and activation dependent variations in muscle shear wave speed. Physiol. Meas. 34, 713–721.

de Vlugt, E., de Groot, J.H., Schenkeveld, K.E., Arendzen, J.H., van der Helm, F.C., Meskers, C.G., 2010. The relation between neuromechanical parameters and Ashworth score in stroke patients. J. NeuroEng. Rehabil. 7, 35.

Ford, L., Huxley, A., Simmons, R., 1981. The relation between stiffness and filament overlap in stimulated frog muscle fibres. J. Physiol. 311, 219–249.

Fortuna, R., Vaz, M.A., Youssef, A.R., Longino, D., Herzog, W., 2011. Changes in contractile properties of muscles receiving repeat injections of botulinum toxin (Botox). J. Biomech. 44, 39–44.

Gao, F., Zhang, L.Q., 2008. Altered contractile properties of the gastrocnemius muscle poststroke. J. Appl. Physiol. 105, 1802–1808.

Gladstone, D.J., Danells, C.J., Black, S.E., 2002. The Fugl-Meyer assessment of motor recovery after stroke: a critical review of its measurement properties. Neurorehabil. Neural Rep. 16, 232–240.

Herzog, W., Powers, K., Johnston, K., Duvall, M., 2015. A new paradigm for muscle contraction. Front. Physiol. 6.

Huxley, A.F., Simmons, R.M., 1971. Proposed mechanism of force generation in striated muscle. Nature 233, 533–538.

Katz, R.T., Rymer, W.Z., 1989. Spastic hypertonia: mechanisms and measurement. Arch. Phys. Med. Rehabil 70, 144–155.

Kojima, H., Ishijima, A., Yanagida, T., 1994. Direct measurement of stiffness of single actin filaments with and without tropomyosin by in vitro nanomanipulation. Proceedings of the National Academy of Sciences 91 (26), 12962–12966.

Koo, T.K., Hug, F., 2015. Factors that influence muscle shear modulus during passive stretch J. Biomech. 48, 3539–3542.

Mathevon, L., Michel, F., Aubry, S., Testa, R., Lapole, T., Arnaudeau, L.F., Fernandez, V., Parratte, B., Calmels, P., 2018. Two-dimensional and shear wave elastography ultrasound: a reliable method to analyse spastic muscles? Muscle Nerve 57, 222–228.

Lacourpaille, L., Hug, F., Bouillard, K., Hogrel, J.Y., Nordez, A., 2012. Supersonic shear imaging provides a reliable measurement of resting muscle shear elastic modulus. Physiol. Meas. 33, N19–N28.

Lamontagne, A., Malouin, F., Richards, C.L., 2000. Contribution of passive stiffness to ankle plantarflexor moment during gait after stroke. Arch. Phys. Med. Rehabil. 81, 351–358.

Lapole, T., Tindel, J., Galy, R., Nordez, A., 2015. Contracting biceps brachii elastic properties can be reliably characterized using supersonic shear imaging. Eur. J. Appl. Physiol. 115, 497–505

Lee, S.S., Spear, S., Rymer, W.Z., 2015. Quantifying changes in material properties of stroke-impaired muscle. Clin. Biomech. 30 (3), 269–275.

Lee, S.S.M., Gaebler-Spira, D., Zhang, L.-Q., Rymer, W.Z., Steele, K.M., 2016. Use of shear wave ultrasound elastography to quantify muscle properties in cerebral palsy. Clin. Biomech. 31, 20–28.

Lieber, R.L., Runesson, E., Einarsson, F., Fridén, J., 2003. Inferior mechanical properties of spastic muscle bundles due to hypertrophic but compromised extracellular matrix material. Muscle Nerve 28, 464–471.

Lieber, R.L., Ward, S.R., 2013. Cellular mechanisms of tissue fibrosis. 4. Structural and functional consequences of skeletal muscle fibrosis. Am. J. Physiol.-Cell Physiol. 305, C241–C252.

Lakie, M., Walsh, E.G., Wright, G.W., 1984. Resonance at the wrist demonstrated by the use of a torque motor: an instrumental analysis of muscle tone in man. J. Physiol. 353, 265–285.

Magid, A., Law, D.J., 1985. Myofibrils bear most of the resting tension in frog skeletal muscle. Science 230, 1280–1282.

Merletti, R., Parker, P.A., 2004. Electromyography: Physiology, Engineering, and Non-Invasive Applications. John Wiley & Sons.

Minajeva, A., Kulke, M., Fernandez, J.M., Linke, W.A., 2001. Unfolding of titin domains explains the viscoelastic behavior of skeletal myofibrils. Biophys. J. 80, 1442–1451.

Muthupillai, R., Lomas, D., Rossman, P., Greenleaf, J., Manduca, A., Ehman, R., 1995. Magnetic resonance elastography by direct visualization of propagating acoustic strain waves. Science 269, 1854–1857.

Nordez, A., Hug, F., 2010. Muscle shear elastic modulus measured using supersonic shear imaging is highly related to muscle activity level. J. Appl. Physiol. 108, 1389–1394.

Pandyan, A., Johnson, G., Price, C., Curless, R., Barnes, M., Rodgers, H., 1999. A review of the properties and limitations of the Ashworth and modified Ashworth Scales as measures of spasticity. Clini. Rehabil. 13, 373–383.

Roy, A., Krebs, H.I., Bever, C.T., Forrester, L.W., Macko, R.F., Hogan, N., 2011. Measurement of passive ankle stiffness in subjects with chronic hemiparesis using a novel ankle robot. J. Neurophysiol. 105, 2132–2149.

Sasaki, K., Toyama, S., Ishii, N., 2014. Length-force characteristics of in vivo human muscle reflected by supersonic shear imaging. J. Appl. Physiol. 117, 153–162.

Singh, P., Joshua, A.M., Ganeshan, S., Suresh, S., 2011. Intra-rater reliability of the modified Tardieu scale to quantify spasticity in elbow flexors and ankle plantar flexors in adult stroke subjects. Ann. Ind. Acad. Neurol. 14, 23.

Sinkjær, T., Magnussen, I., 1994. Passive, intrinsic and reflex-mediated stiffness in the ankle extensors of hemiparetic patients. Brain 117, 355–363.

Takebayashi, T., Morita, Y., Oosawa, F., 1977. Electronmicroscopic investigation of the flexibility of F-actin. Biochimica et Biophysica Acta (BBA)-Protein Struct. 492, 357–363.

Yoshitake, Y., Takai, Y., Kanehisa, H., Shinohara, M., 2014. Muscle shear modulus measured with ultrasound shear-wave elastography across a wide range of contraction intensity. Muscle Nerve 50 (1), 103–113.